22 Sep 2020

Hybrid Electro-Plasmonic Neural Stimulation with Visible-Light-Sensitive Gold Nanoparticles

Ratka Damnjanovic

Parveen Bazard
Missouri University of Science and Technology, parveen1@usf.edu

Robert D. Frisina

Venkat R. Bhethanabotla

Recommended Citation

R. Damnjanovic et al., "Hybrid Electro-Plasmonic Neural Stimulation with Visible-Light-Sensitive Gold Nanoparticles," *ACS Nano*, vol. 14, no. 9, pp. 10917 - 10928, American Chemical Society, Sep 2020.
The definitive version is available at https://doi.org/10.1021/acsnano.0c00722

ACS NANO

www.acsnano.org

ARTICLE

Hybrid Electro-Plasmonic Neural Stimulation with Visible-Light-Sensitive Gold Nanoparticles

Ratka Damnjanovic, Parveen Bazard, Robert D. Frisina,* and Venkat R. Bhethanabotla*

Cite This: *ACS Nano* 2020, 14, 10917−10928

Read Online

ACCESS | Metrics & More | Article Recommendations

ABSTRACT: Biomedical prosthetics utilizing electrical stimulation have limited, effective spatial resolution due to spread of electrical currents to surrounding tissue, causing nonselective stimulation. So, precise spatial resolution is not possible for traditional neural prosthetic devices, such as cochlear implants. More recently, alternative methods utilize optical stimulation, mainly infrared, sometimes paired with nanotechnology for stimulating action potentials. Infrared stimulation has its own drawbacks, as it may cause collateral heating of surrounding tissue. In previous work, we employed a plasmonic method for stimulation of an electrically excitable neuroblastoma cell line, which had limited success. Here, we report the development of a hybrid electro-plasmonic stimulation platform for spatially and temporally precise neural excitation to address the above deficiencies. Primary trigeminal neurons were costimulated *in vitro* in a whole-cell patch-clamp configuration with subthreshold-level short-duration (1−5 ms) electrical and visible light pulses (1−5 ms). The visible light pulses were aimed at a gold-nanoparticle-coated nanoelectrode placed alongside the neuron, within 2 μm distance. Membrane action potentials were recorded with a 3-fold higher success rate and 5-fold better poststimulation cell recovery rate than with pure optical stimulation alone. Also, electrical stimulus current input was being reduced by up to 40%. The subthreshold levels of electrical stimuli in conjunction with visible light (532 nm) reliably triggered trains of action potentials. This single-cell hybrid activation was reliable and repeatable, without any damage as observed with pure optical stimulation. This work represents an empirical cellular study of the membrane action potential response produced by the cultured primary sensory trigeminal neurons when costimulated with plasmonic and electrical (hybrid) stimulation. Our hybrid neurostimulation method can be used toward development of high-acuity neural modulation prosthetic devices, tunable for individual needs, which would qualify as a preferred alternative over traditional electrical stimulation technologies.

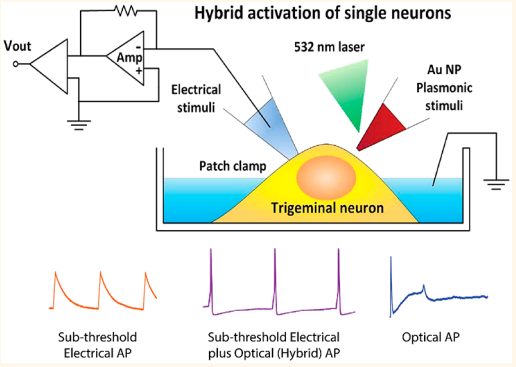

KEYWORDS: *neuromodulation, electro-plasmonic hybrid stimulation, gold nanoparticles, localized surface plasmon resonance, visible light, trigeminal neurons, cochlear implants*

Electrical stimulation, although successful at activating neural responses, tends to spread to surrounding tissues, resulting in nonspecific stimulation, making it difficult to stimulate discrete neural sites. To facilitate specific point stimulation, various nanomaterial-assisted neural stimulation approaches have been reported in recent years[1−4] where different localized fields are activated (electric, magnetic, thermal) employing different nanomaterials for stimulation, such as piezoelectric ultrasound waves,[5] magnetic fields,[6] and laser light electromagnetic waves (mainly near-infrared[7−11] and infrared[12]) optical irradiation.

Optical stimulation approaches mainly rely on top-down methodology focused on recording outputs in response to a stimulation input, such as observing muscle contraction as a result of the triggered action potential (AP) response in various animal subjects.[13] More recently, there have been reports of optical stimulation performed in brain tissue slices[14] as well as single-cell stimulation of cultured neurons (dorsal

Received: January 26, 2020
Accepted: June 30, 2020
Published: June 30, 2020

https://dx.doi.org/10.1021/acsnano.0c00722
ACS Nano 2020, 14, 10917−10928

root ganglion,[4,15] spiral ganglion,[16] hippocampal neurons,[17] oocytes[18]). A common approach has been to use infrared (IR) light wavelengths[19] to heat the surrounding aqueous medium sufficiently to induce fast changes in the temperature of the local surroundings, which can heat and stimulate the cell's membrane, presumably triggering membrane capacitive currents.[18]

Although direct heating of the bulk solution has been shown to be effective in triggering action potentials, it is an imprecise way to stimulate neurons, as it heats nonspecifically and may cause cellular damage. Attempts have been made to modify the stimulation methods and utilize localized surface plasmon resonance (LSPR) fields for more target-specific heating. Nanoparticle techniques, such as functionalization, bioconjugation, local injection and deposition of nanoparticles to the target site, have been attempted.[4] For example, Parameswaran *et al.*[15] demonstrated that cathodic photocurrents from single nanowires can elicit action potentials in primary rat dorsal root ganglion (DRG) neurons through a primarily atomic gold-enhanced photoelectrochemical process using coaxial p-type/intrinsic/n-type (PIN) silicon nanowires (SiNWs). Upon optical stimulation with 532 nm light illumination at the neuron/PIN-SiNW interface, electrons move toward the n-type shell and holes to the p-type core, inducing a Faradaic cathodic process at the n-shell that locally depolarized the target neuron. Carvalho-de-Souza *et al.*[4] conjugated Au nanoparticles with three different ligands—Ts1 neurotoxin and two antibodies (targeting TRPV1 and $P2X_3$ channel receptors, respectively)—and successfully bound the particles to dorsal root ganglion neurons, then stimulated the DRGs with 532 nm green laser light. Nakatsuji *et al.*[20] presented a method using plasma-membrane-targeted gold nanorods (pm-AuNRs) prepared with a cationic protein/lipid complex to activate a thermosensitive cation channel, TRPV1, in intact neuronal cells by using near-infrared (NIR) light. In this study, the highly localized photothermal heat generation mediated by the pm-AuNRs induced Ca^{2+} influx solely by TRPV1 activation. Eom *et al.*[7] conjugated Au nanorods by injection into the rat sciatic nerve using a glass pipet and then excised the nerve bundle and recorded compound nerve action potentials in response to 980 nm IR laser stimulation. Recently, it has been shown that neural cells can be activated more efficiently by pulsed NIR light delivered to gold nanorods (GNRs) near the neural cells, but the mechanisms underlying this GNR-enhanced NIR stimulation have not been explained yet. Eom *et al.*[21] proposed a model to elucidate the mechanisms by modeling the heat generated from interactions between NIR light and GNRs, the temperature-dependent ion channels (transient receptor potential vanilloid 1; TRPV1) in the neuronal membrane, and a heat-induced capacitive membrane current. Their results show that NIR pulses induce rapid temperature increases near the neural membrane triggering TRPV1 channel currents and capacitive currents. Both currents collectively increase the generator potential, eliciting an action potential, and the stimulus conditions determine which source will be the dominant mechanism, such as the laser pulse duration or the TRPV1 channel density. They concluded that, although the TRPV1 mechanism dominates in most cases, the capacitive current has a greater contribution when a very short laser pulse is used for neural cells with relatively low TRPV1 channel densities. Yoo *et al.*[10] performed coating of Au nanorods with polyethylene glycol (PEG) to assist binding to the cell membrane and then invoked inhibition in the rat hippocampal tissue using a 785 nm NIR laser. Li *et al.*[11] utilized photosensitive hydrogels embedded with polypyrrole (PPy) nanoparticles to release biomolecule transmitters (glutamate and DNQX) and then used 980 nm IR laser light to excite hippocampal neurons *in vitro* when glutamate was released and to inhibit responses from the rat visual cortex *in vivo* when DNQX was released. Yong *et al.*[8] incubated primary auditory neurons with silica-coated Au nanorods overnight and used a 780 nm NIR laser to excite the neurons. A common theme for these studies is that they employ various modifications of nanoneural interfaces to achieve optical stimulation. The major limitation with these techniques is that they have issues regarding unwanted toxicity, biocompatibility, and repeatability. For instance, excessive heating by IR lasers to excite neurons can damage healthy tissues. Therefore, there is a need to find more suitable ways for conversion into neural prosthetics that would minimize cellular and surrounding tissue damage.

Here, we use an Au nanoelectrode (AuNPs-coated borosilicate glass micropipet), which did not need any bioconjugation or surface modifications of the nanoneural interface to achieve neural excitation. This nanoelectrode was characterized and validated for generation of plasmonic responses in our previous work, Bazard *et al.*,[22] by stimulating two different types of cells, SH-SY5Y human neuroblastoma cell line, which has characteristics of neurons, and neonatal cardiomyocytes. The present work investigated whether electro-plasmonic co-stimulation at the subthreshold level could modulate single-cell neural activity of primary neurons and more specifically trigeminal neurons. We evaluated how visible green light (532 nm, 1−5 ms pulses) could be used to stimulate primary neurons in conjunction with reduced levels of electrical stimulation. Like our previous report,[22] there was success with pure optical stimulation, but a minority of cells responded to the optical stimuli alone, and detrimental effects were generally observed on cells with higher power levels of pure optical stimulation. To overcome these shortcomings, we used short-duration optical stimulation in conjunction with subthreshold level electrical stimuli, to consistently activate primary neurons and for improved success rates, repeatability, and reproducibility. These findings serve as an initial *in vitro* proof of concept for optical plasmonic stimulation of primary neurons, and more specifically trigeminal neurons, using the LSPR phenomena. This was achieved by illuminating the AuNPs-coated nanoelectrode, positioned within 2 μm from the neuron, with a 532 nm green laser light. The present study further expands employment of hybrid electro-plasmonic stimulation to elicit AP responses in primary trigeminal neurons. We also showed how various combinations of pulse durations, through repetitive bursts of electrical and plasmonic pulses at the subthreshold level, modulate neural firing patterns in primary neurons to achieve cellular AP responses with improved firing success rates, survival rates, and repeatability, while significantly reducing the negative side effects, such as the overheating of surrounding tissue as reported with IR laser light or the poor specificity as with electrical stimulation alone.

We chose the trigeminal nerve for culturing neurons due to its wide array of functions. The trigeminal nerve is the fifth cranial nerve and the principle sensory nerve of the head that innervates the nasal cavity, paranasal sinuses, oral mucosa, and the skin of the face, as well as the cerebral arteries and the dura mater. As such, the trigeminal neuron has mixed sensory, motoric, and parasympathetic functions, with a large sensory

https://dx.doi.org/10.1021/acsnano.0c00722
ACS Nano 2020, 14, 10917−10928

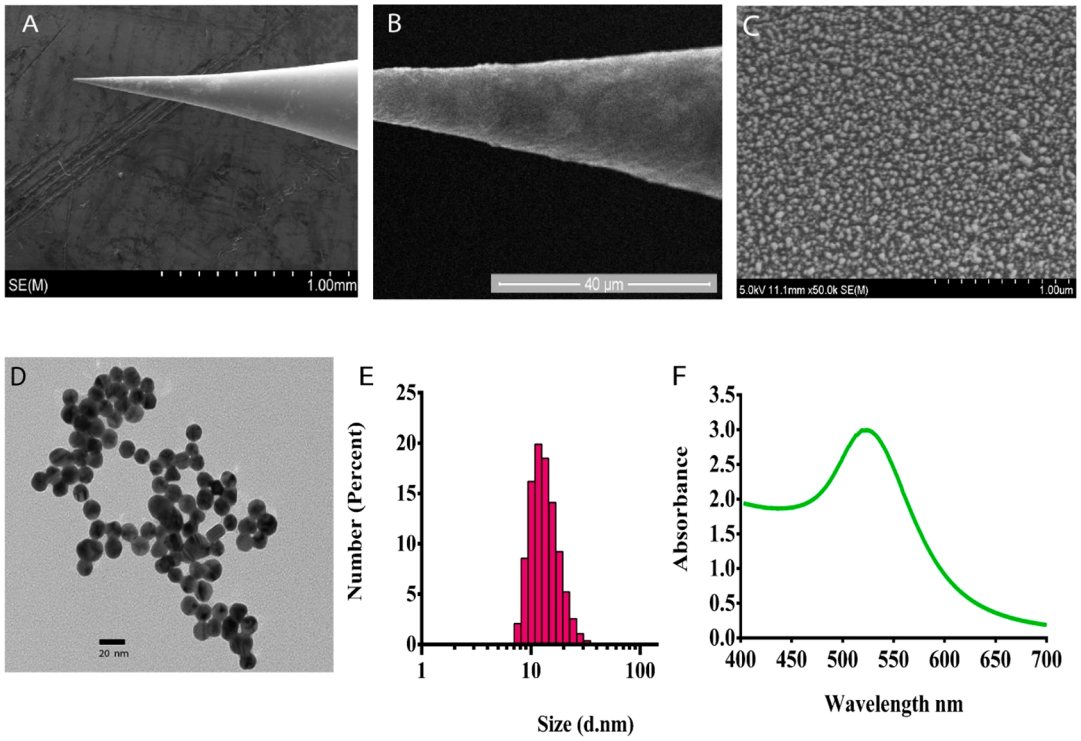

Figure 1. Characteristics of the nanoplasmonic nanoelectrode. (A, B, and C) SEM images of the nanoelectrode, whose tip was coated with ~20 nm diameter colloidal gold nanoparticles (AuNPs). (D) TEM image of the AuNP suspension, which was synthesized using a liquid phase method by adding 2−3 mL of a 1% solution of trisodium citrate to a boiling $HAuCl_4 \cdot 3H_2O$ solution, under continuous stirring, and boiled until it turned maroon red in color, indicating the presence of AuNPs. (E) Particle size distribution histogram by number (percent) of the synthesized AuNPs, determined using a Zetasizer particle counter. (F) LSPR absorption spectrum of the AuNPs, with a maximum peak value around the 520 nm wavelength, determined using a PerkinElmer Lambda 35 UV/vis spectrophotometer (190−1100 nm wavelength range, 0.5−4 nm variable bandwidth range) to obtain the UV/vis absorption spectra of the AuNP solution.

root and a smaller motor root, which sprout from the side of the pons into three branches as follows: (1) ophthalmic (CN V1) and (2) maxillary (CN V2) general sensory components and (3) mandibular (CN V3) general sensory and branchial motor components.[23] The trigeminal nerve is in constant communication with the autonomic nervous system, including the ciliary, sphenopalatine, otic, and submaxillary ganglia and the oculomotor, facial, and glossopharyngeal nerves.[24] In addition, the trigeminal nerve conveys information to key areas in the brain, including the locus coeruleus, the nucleus solitarius, the vagus nerve, and the cerebral cortex. The trigeminal nerve also sends signals to the anterior cingulate cortex, which is involved in attention, mood, and decision-making.

RESULTS AND DISCUSSION

To investigate whether the activity of a single primary neuron can be evoked by plasmonic and hybrid stimulation, an *in vitro* patch-clamp electrical and optical stimulation and recording platform was utilized. Plasmonically evoked APs were recorded in response to laser stimulation with a 50 μm diameter optical fiber (green, 532 nm, 1−5 ms pulses, laser power 75−125 mW). The coating uniformity of the AuNPs-coated nanoelectrode surface was verified using scanning electron microscopy (SEM) imaging (Figure 1A, B, and C). The colloidal AuNP diameters displayed a normal distribution around 10−20 nm, as shown in the transmission electron microscopy (TEM) imaging and in the particle size distribution histogram obtained using a Zetasizer particle counter (Figure 1D and E). A visible color change of the gold solution from yellow to reddish-maroon was observed during synthesis, and a strong LSPR absorption spectrum using UV−visible spectroscopy had a maximum peak value at the 520 nm wavelength, indicating the formation of AuNPs (Figure 1F). Initial neural stimulation experiments were performed to establish a baseline for LSPR-enabled plasmonic stimulation thresholds. All electrophysiological experiments were done in a whole-cell patch-clamp configuration (Figure 2). The individual trigeminal neurons were patch-clamped in the standard whole-cell current clamp configuration using a patch-clamp electrode and then transiently exposed to a 532 nm laser pulse (100 mW power, 5 ms pulse duration) aimed at the tip of a AuNPs-coated micropipet positioned next (within 2 μm distance) to the patched trigeminal neuron cell (Figure 2). The holding current was adjusted to the minimum threshold value in order to set the membrane potential to a baseline value (around −70 mV). The trigeminal cells were stimulated with depolarizing electrical currents to trigger a control AP and verify that cells were electrically excitable before proceeding to plasmonic excitation. Then the patch-clamped trigeminal neuron was stimulated with visible 532 nm wavelength light delivered from an optical fiber at 75−125 mW laser power for 1−5 ms duration, by shining the laser beam at the tip of a AuNPs-coated micropipet positioned next to the patched neuron, within 2 μm distance. The presence of the AuNPs-coated nanoelectrode, in the close vicinity of the neurons, enabled responses to the applied 75−125 mW, 1−5 ms laser pulses, but with very limited success. A fraction of the

https://dx.doi.org/10.1021/acsnano.0c00722
ACS Nano 2020, 14, 10917−10928

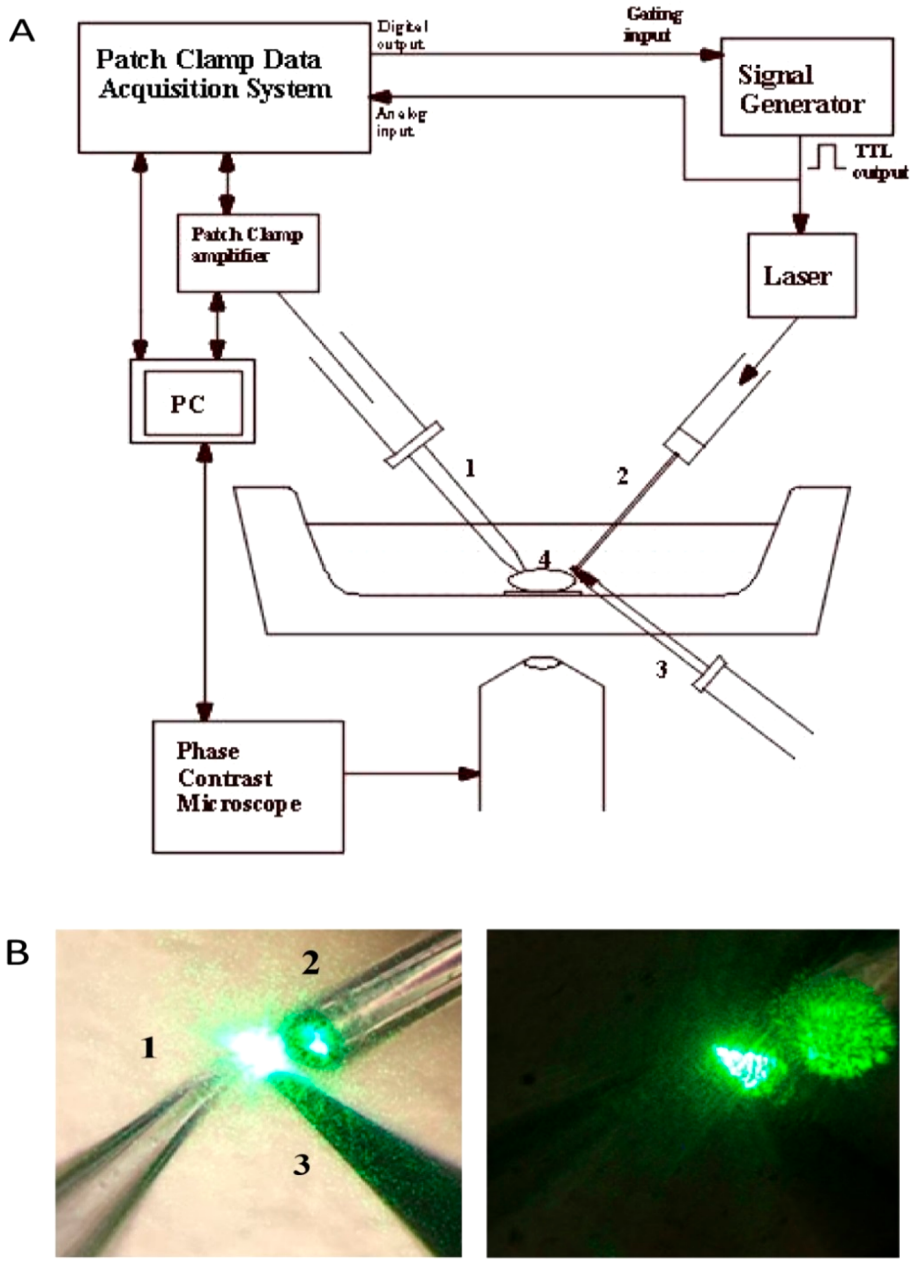

Figure 2. Schematic and digital pictures of the experimental patch-clamp setup. (A) Whole-cell patch-clamp technique used in conjunction with an Axopatch 700B Multiclamp amplifier connected to a patch pipet filled with an intracellular solution (ICS), known as the measuring electrode (1), paired with a Digidata 1440A data acquisition interface (Molecular Devices) and pCLAMP-9 software (Axon Instruments, Union City, CA, USA). Extracellular solution (ECS) was used to flood the cells (4) in the Petri dish. A 50 μm inside diameter optical fiber (2) was used to focus a 532 nm green laser light onto the surface of the Au-nanoparticles (AuNPs)-coated nanoelectrode tip (3). The AuNPs-coated nanoelectrode was placed near the cell's surface (~2 μm). For the hybrid stimulation, an electrical stimulus was added *via* the patch-clamp electrode (1), in addition to the optical plasmonic stimulation generated by the laser beam (2) from the optical fiber (ThorLabs) shining onto the tip of the AuNPs-coated nanoelectrode (3). Neural responses were recorded using the patch-clamp electrode (1). (B) Digital micrographs of the experimental patch-clamp setup when illuminated by the laser beam, inducing the plasmonic effect at the AuNPs-coated nanoelectrode tip, as seen inside the Petri dish under 5× (left) and 20× (right) magnifications.

stimulated cells (6 out of 23) produced AP responses with pure optical stimulation, while the rest of the cells responded with only a shift in membrane potential or an incomplete/partial repolarization only. Representative traces of the current-clamped trigeminal neurons (N = 4) and firing action potentials in response to the plasmonic stimulation are presented in Figure 3A (middle). It was observed that the pure optical (plasmonic) APs were smaller in magnitude compared to the pure electrical (preplasmonic) APs. Also, it was noticeable that the postplasmonic APs (Figure 3A, right), recorded when cells were stimulated with electric current pulses of the same magnitude (150 pA, 300 ms) as in the preplasmonic electrical stimulation (Figure 3A, left), resulted in APs with significantly smaller amplitude than the original electrical APs. Also, one of the four cells did not survive the plasmonic stimulation; therefore, it could not produce a postplasmonic electrical AP. Plasmonic action potentials were not consistent, in terms of amplitude and timing, like

https://dx.doi.org/10.1021/acsnano.0c00722
ACS Nano 2020, 14, 10917−10928

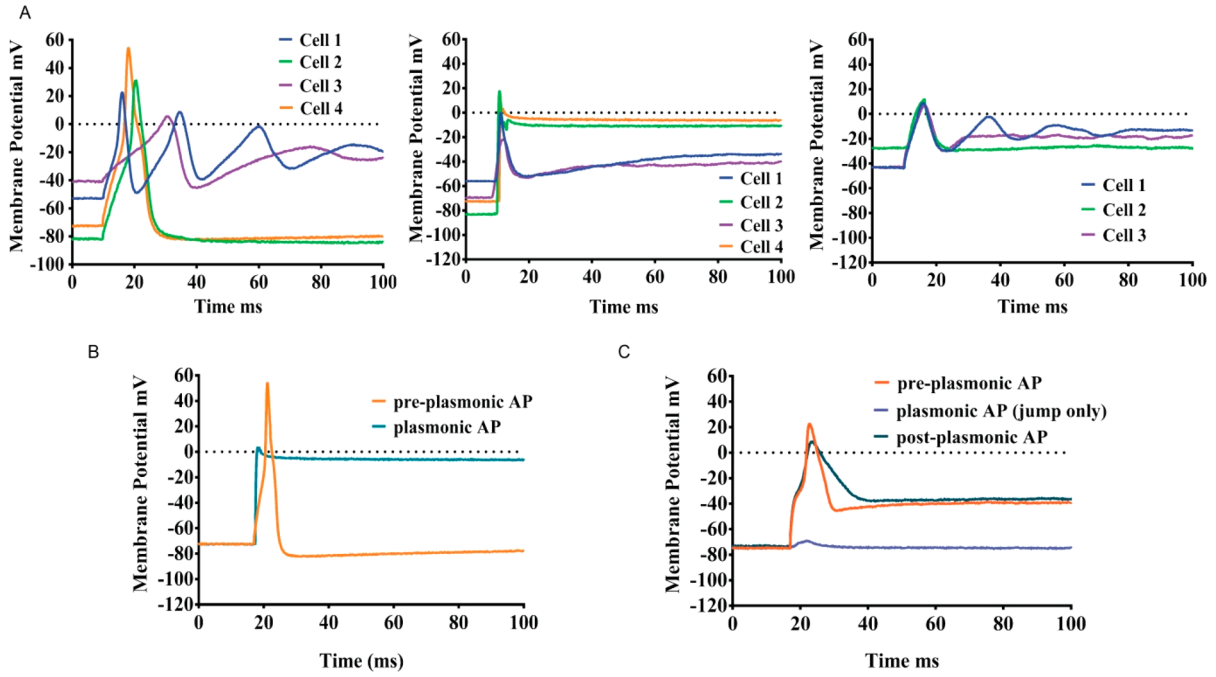

Figure 3. Plasmonic stimulation of primary mouse trigeminal neurons: whole-cell current-clamp recordings. Current-clamp recordings of the membrane potential (mV) in trigeminal neurons elicited by shining green laser light (532 nm) at 100 mW power and 5 ms pulse duration onto the surface of a AuNPs-coated micropipet positioned ~2 μm from the cell. (A) Four representative cells excited by plasmonic neural stimulation. Left: Electrical stimulation APs (preplasmonic) recorded when cells were stimulated with electric current pulses (150−300 pA, 300 ms): control condition. Middle: Plasmonic stimulation APs recorded when cells were stimulated for 1−5 ms by green laser pulses (75−120 mW laser power). The pure optical (plasmonic) APs were smaller in magnitude compared to the pure electrical (preplasmonic) APs. Right: Electrical stimulation APs (postplasmonic) recorded when cells were stimulated with electric current pulses of the same magnitude as in the preplasmonic electrical stimulation (min 150−300 pA, 300 ms). These postplasmonic APs were recorded with significantly smaller amplitudes than the preplasmonic APs. One of the cells did not survive the plasmonic stimulation; therefore it could not produce a postplasmonic electrical AP. (B) Type 1: Typical plasmonic stimulation AP response of trigeminal neurons in a whole-cell current-clamp recording where the cell is not responsive to postplasmonic electrical stimulation. The majority of plasmonic stimulation attempts (approximately 80%) result in this type of AP response. This was likely related to cell membrane damage due to plasmonic exposure, manifested in the premature termination or leveling out of the AP response into a termination peak immediately after the depolarization phase, with no evident repolarization. In those terminated cells, the postplasmonic electrical stimulation AP response was often not possible, as the cell's membrane damage led to no physiological response. (C) Type 2: The second most typical plasmonic stimulation AP response of trigeminal neurons in a whole-cell current-clamp recording is where the cell is only partially responsive to optical stimulation. A weak membrane potential shift (10−20 mV jump) occurred, not a complete AP, or the cell was completely irresponsive to the plasmonic stimulus following a successful preplasmonic electrical stimulation AP. In those irresponsive cells, the postplasmonic electrical stimulation AP response had a slightly smaller amplitude, compared to the preplasmonic electrical stimulation AP response, and it lacked repolarization acuity.

electrically induced APs. While laser light between 75 and 125 mW power was sufficient to reliably trigger APs, two characteristic types of membrane potential outputs were observed. Type 1 is the characteristic output when the trigeminal neuron cell depolarizes, with no/negligible repolarization of APs following optical laser plasmonic stimulation (Figure 3B). Approximately 80% of plasmonic stimulation attempts (8 out of 10 cells) resulted in this type of AP response. This outcome implies cell membrane damage due to plasmonic exposure or passivation resulting in ion channel dysfunction, which plays a principal role in regulating cellular excitability and whose damage or misbalance can cause irregular depolarization and repolarization patterns. This is manifested in the premature termination or leveling out of the AP response peak, immediately after firing the plasmonic triggered AP discharge, with no/minimal evident repolarization down-slope once reaching the peak. In those cells, the postplasmonic electrically evoked AP response typically returned to normal, after a short resting period (few seconds to minutes). In some cases though, the postplasmonic electrical stimulation was not possible, as the cell membrane demonstrated persistently prolonged passive behavior after an optically induced AP from pure plasmonic stimulation. Similar behavior was reported by researchers who studied effects of AuNPs-aided stimulation of DRG neurons following a laser pulse, indicating cell damage was frequently observed following an AP, resulting in loss of excitability.[4] Type 2 is the characteristic output when the cell is partially responsive to optical stimulation right from the start, following a successful preplasmonic electrical stimulation AP firing (Figure 3C). In response to the optical stimulation, cells produce only a very weak membrane potential shift (only a 10−20 mV jump), therefore not a complete AP. This can be partially dependent on the nanoelectrode positioning and proximity to the cell (nanoelectrode tip must be next to the cell (<2 μm distance) and laser beam clearly focused on the tip of the nanoelectrode to get sufficient thermal effects in order to produce plasmonic excitation results), as well as the laser power. It was observed that laser power of <75 mW directed at the surface of the AuNPs-coated nanoelectrode was insufficient to stimulate the

https://dx.doi.org/10.1021/acsnano.0c00722
ACS Nano 2020, 14, 10917−10928

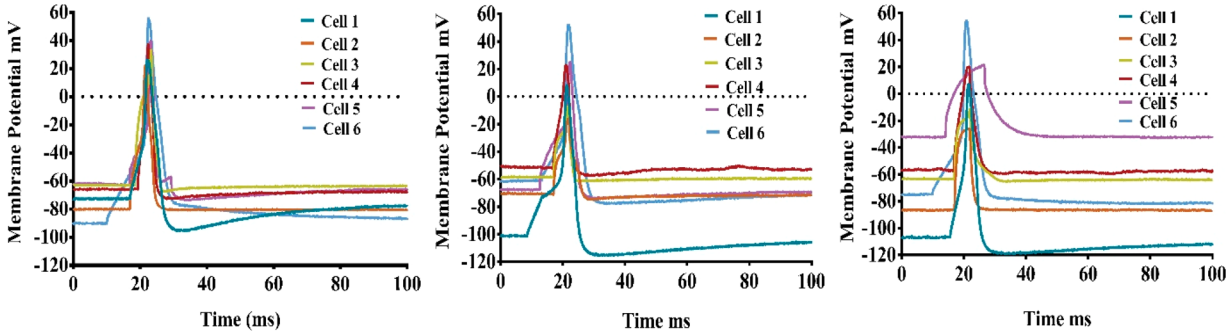

Figure 4. Hybrid electro-plasmonic stimulation results: whole-cell current-clamp recordings. Membrane APs of trigeminal neurons subjected to an electro-plasmonic (hybrid) stimulus in a whole-cell current-clamp recording for six different trigeminal neurons. Left: Electrical stimulation APs (prehybrid) recorded when cells were stimulated with electric current pulses (min 150 pA, 5 ms): control conditions. Middle: Electro-plasmonic (hybrid) stimulation APs recorded when the cells ($N = 6$) were stimulated with the combined 1−5 ms, 532 nm green laser pulses and subthreshold electric current pulses at reduced levels. When short-duration laser pulses (1−5 ms) were superimposed with electric current pulses, APs were reliably recorded from trigeminal neurons. Peak responses recorded with hybrid stimulation were higher than pure optical stimulation (Figure 3A) by 10 to 20 mV on average. Right: Posthybrid electrical stimulation recordings when cells were stimulated with electric current pulses of the same magnitude as in prehybrid stimulation. Cells made consistently similar AP responses as the original values observed from the initial electrical (prehybrid) stimulation.

cells. A laser power between 75 and 125 mW was sufficient to generate the plasmonic effect and evoke an AP response in the trigeminal neurons. Some cells (approximately 2 out of 10 cells) had a type 2 profile of a suppressed membrane potential response when subjected to plasmonic stimulation. These cells recover quickly and are able to fire full AP in response to an electrical stimulation afterward. Most plasmonic stimulated APs had good depolarization but diminished repolarization peak-to-valley return (~20%) as compared to the original electrically triggered preplasmonic APs. This effect lasted, as the diminished repolarization is also noticeable when the cells are electrically stimulated postplasmonic stimulation. This indicates temporary impairment or permanent irreversible damage of the cell membrane caused by the pure plasmonic stimulation. This side effect is consistent with the literature, in that plasmonic stimulation results in a reluctance of the cell to recover quickly and fully to its original base state in a short amount of time once the heat is discontinued.[4,22] We observed recovery time for the membrane to return to its original preplasmonic excitability or resting potential state to be a few seconds to a minute. This could be due to an increased tendency for cellular damage as a consequence of the local photothermal effects.

To address the shortcomings of pure optical stimulation, we hypothesized that the combination of optical stimulation with subthreshold levels of electrical stimulation will avoid damaging the cells. Hence, next, we employed a combined electrical and optical stimulation procedure to utilize the advantages of both stimulation modes and to introduce the ability to turn on and off individual neurons by fine-tuning the proposed hybrid stimulation (combined optical and electrical). We also optimized the neural outputs with various combinations of short-duration repetitive bursts of electro-plasmonic pulses to modulate neural firing patterns. These results provide a proof of concept for using this type of hybrid electro-plasmonic stimulation to elicit APs in primary neurons, and more specifically trigeminal neurons.

Representative traces of the current-clamped trigeminal neurons show firing APs in response to the hybrid stimulation, when cells were stimulated with the combined 1−5 ms, 532 nm green laser pulses and a subthreshold electrical current pulses at reduced levels (Figure 4, middle). Observe that the recorded hybrid stimulation APs, when short-duration laser pulses (1−5 ms) were combined with electric current pulses, were comparable in magnitude as well as timing to the pure electrical (prehybrid) APs. Further, the peak responses recorded with hybrid stimulation were higher than the previously recorded peak responses with pure optical stimulation alone, by 10 to 20 mV. In addition, the posthybrid APs (Figure 4, right), recorded when cells were stimulated with electric current pulses of the same magnitude (min 150 pA, 5 ms) as in the initial prehybrid electrical stimulation (Figure 4, left), resulted in APs with comparable amplitude to the original electrical APs. Also, all cells survived the hybrid stimulation and did produce posthybrid electrical stimulation APs (Figure 4, right), unlike postplasmonic stimulation (Figure 3A, right). This survival rate was higher as compared to after pure plasmonic stimulation, most likely because there was no membrane damage. It is likely that pairing the short-duration green light pulse stimulus with electrical current pulses aids electrically excitable ion-gate activation in addition to the plasmonically triggered photothermal activation effects. So, these two stimuli have mutually beneficial additive effects on the resulting AP responses.

The mean plasmonic AP responses and the mean hybrid (electro-plasmonic) AP responses were further compared for variation and profiling (Figure 5A and B). The electrical stimulus amplitude required to evoke APs was reduced by 33−38% when a plasmonic stimulus (1−5 ms pulse width) is added to the electrical input, compared to electrical stimulation alone (Figure 5C). We also observed that this hybrid neural stimulation has no deleterious effects on the neurons; that is, the cells fired electrical stimulated APs immediately after the hybrid stimulation, unlike the pure optical stimulation approach alone (reported above). The observed plasmonic *vs* hybrid stimulation AP success rates were 26% ($N = 23$) for plasmonic *vs* 83% ($N = 29$) for hybrid stimulation of the trigeminal neurons, so 3 times the success rate when stimulating with hybrid stimulation *vs* plasmonic (Figure 5D). The observed plasmonic *vs* hybrid survival rates were 13% ($N = 23$) postplasmonic *vs* 72% ($N = 29$) of trigeminal neurons posthybrid APs. Therefore, an order of magnitude >5.5× for the survival rate of trigeminal neurons when

https://dx.doi.org/10.1021/acsnano.0c00722
ACS Nano 2020, 14, 10917−10928

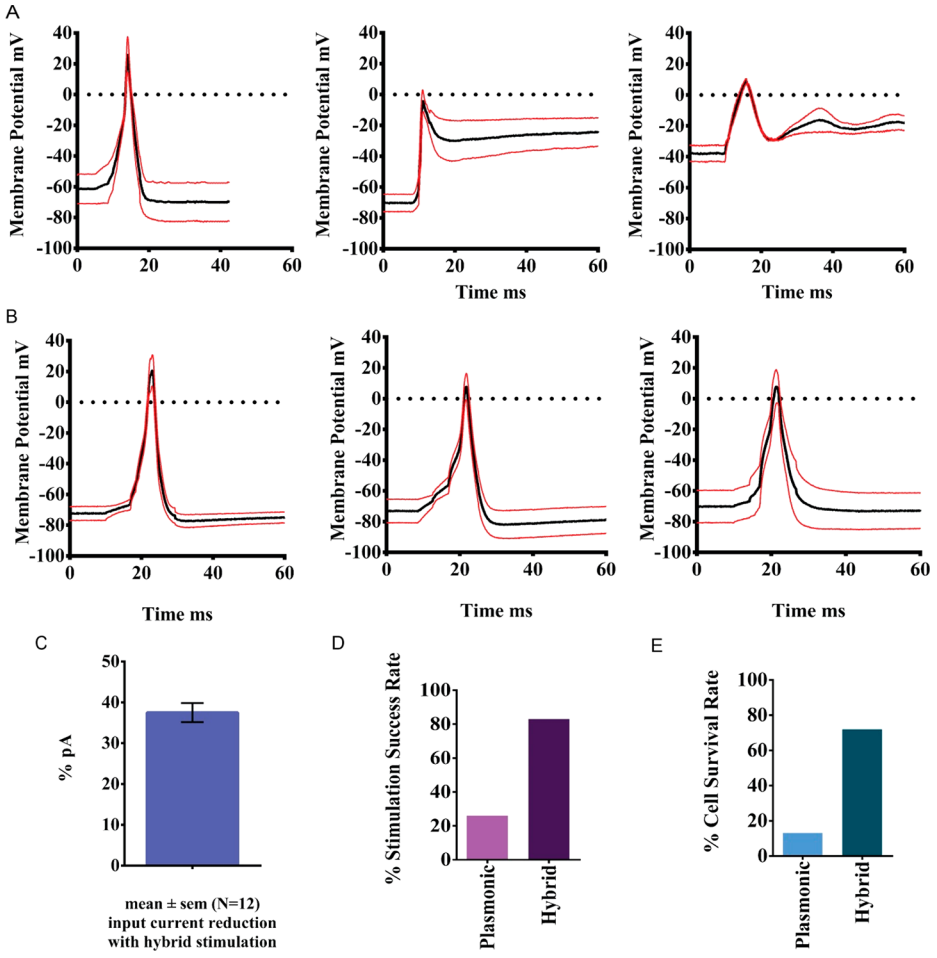

Figure 5. Comparison of plasmonic *vs* hybrid stimulation results of primary mouse trigeminal neurons: whole-cell current-clamp recordings. (A) Mean plasmonic electrophysiology AP responses (N = 4). Left: Preplasmonic electrical AP responses. Middle: Plasmonic AP response. Right: Postplasmonic electrical AP response. (B) Mean hybrid (electro-plasmonic) AP responses (N = 6). Left: Prehybrid electrical AP responses. Middle: Hybrid (electrical + optical) AP responses. Right: Posthybrid electrical AP responses. (C) Mean input current reduction (% pA) as observed in (N = 12) trigeminal cells when stimulated with hybrid electro-plasmonic stimulation *vs* pure electrical current stimulation. The current reduction is 38 ± 2%. (D) Plasmonic *vs* hybrid stimulation success rate. Success rate is defined as the ratio of the number of successful pure optical (or hybrid) stimulation APs *vs* the total number of cells stimulated with optical (or hybrid) stimulation, respectively. Observed AP success rates were 26% (N = 23) for plasmonic *vs* 83% (N = 29) for hybrid stimulation, for cells that previously produced electrically stimulated baseline APs. The hybrid stimulation success rate is an order of magnitude >3 as compared to the plasmonic stimulation success rate. (E) Plasmonic *vs* hybrid survival rate. Observed neuron survival rates were 13% (N = 23) of trigeminal neurons after plasmonic stimulation *vs* 72% (N = 29) of trigeminal neurons after hybrid stimulation. The hybrid stimulated trigeminal neurons' survival rate is an order of magnitude >5.5 compared to the plasmonic stimulated trigeminal neurons' survival rate.

stimulated with hybrid stimulation compared to plasmonic alone (Figure 5E).

Further optimization experiments were carried out to study the lead- and lag-time effects of electrical *vs* plasmonic pulses in a hybrid electro-plasmonic stimulation combo on AP generation. Electro-plasmonic hybrid stimulation (5 ms; 75–120 mW, 532 nm) pulses were presented to trigeminal neurons at subthreshold electrical input currents. We found that a lead or lag time greater than 2.0 ms, of either electrical or optical pulse in reference to each other, did not produce regular shape APs; there was only a shift in membrane potentials. An optical lead of up to 0.6 ms before electrical pulses produced standard APs. Electrical lead times of as low as 0.4 ms before optical and up to 1.4 ms before optical also produced good hybrid APs (Figure 6A). We concluded that electrical pulse leads of <1 ms before optical was the best condition to excite neurons. In additional experiments, the optical pulse duration (1 ms) was fixed and the electrical pulse duration was varied, from 1 to 5 ms, at the hybrid subthreshold intensity level, where the electrical pulse preceded the optical pulse by 0.7 ms. AP peak responses increased as the subthreshold electrical pulse duration increased, as shown in a representative hybrid stimulation of a primary trigeminal neuron (Figure 6B). The difference (delta) between the AP peak value and base value (first minimum after peak) increased with pulse duration increases, due to the increase in the AP peak maxima as well as the increase in the hyperpolarization, resulting in full AP responses for pulses between 3 and 5 ms in duration.

Our findings further show the applicability of short-duration pulses (1–5 ms) when applied repeatedly, for subthreshold electrical and LSPR visible light stimulation pulses, in combination with AuNPs-coated substrates (nanoelectrodes), for obtaining repeatable multiple trains of APs from neurons (Figure 6C). Neural cell survival rates and viability after hybrid stimulation were superior to that of pure optical stimulation. The input current sufficient to trigger APs with multiple hybrid

https://dx.doi.org/10.1021/acsnano.0c00722
ACS Nano 2020, 14, 10917–10928

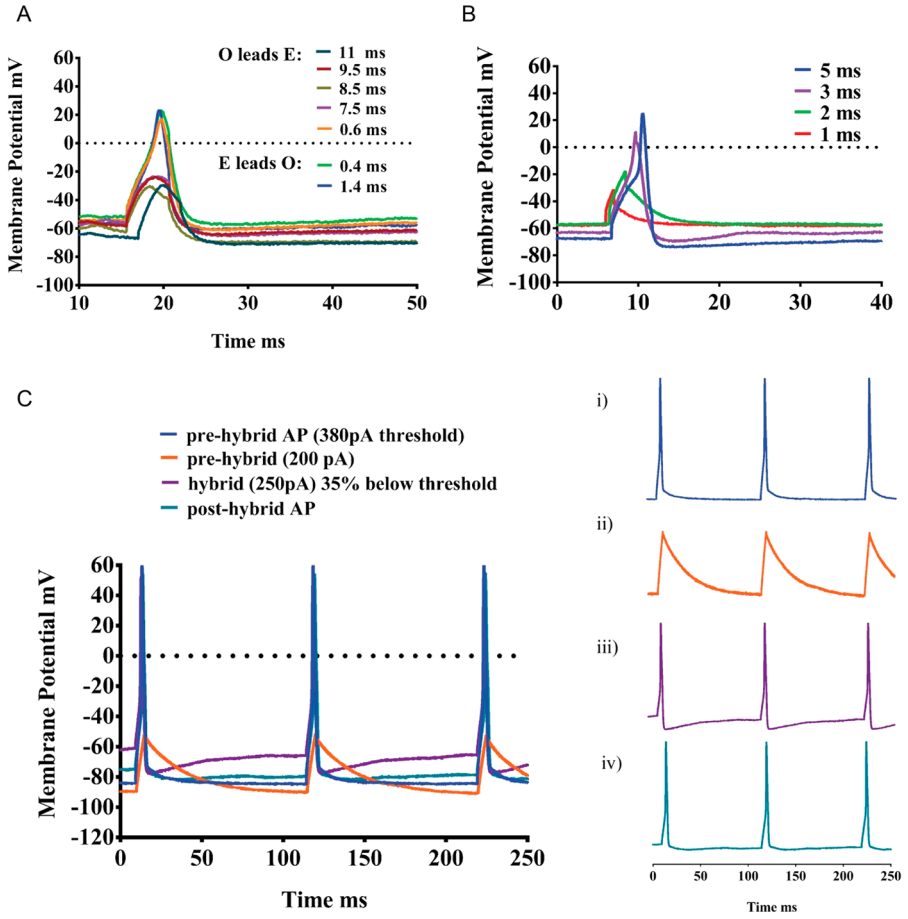

Figure 6. Optimization of hybrid stimulation opto-electric parameters. (A) Lead and lag time effects of electrical *vs* plasmonic pulses for our hybrid electro-plasmonic stimulation paradigm. Electro-plasmonic hybrid stimulation (5 ms; 75−120 mW, 532 nm) pulses were applied at a subthreshold electrical input current. The shift in membrane potential indicates that a lead or lag time greater than 1.4 ms, of either electrical or optical pulse in reference to each other, did not produce standard neural stimulation AP responses. Optical lead of up to 0.6 ms before electrical as well as electrical lead of up to 1.4 ms before optical both produced good hybrid APs. (B) At a fixed optical pulse duration (1 ms), hybrid subthreshold electrical stimulation was varied from 1 to 5 ms, where the electrical pulse leads the optical by 0.7 ms in time of initiation. AP peak responses increased as the subthreshold electrical pulse duration increased, with a pulse duration of 3−5 ms being the optimal for getting full AP response from the neuron. The difference (delta) between the AP peak value and base value (first minima after peak) increased with the pulse duration increase, where the increase is greater when the pulse durations exceeds 3 ms, due to the increase in the AP peak values as well as the increase in the hyperpolarization minima. (C) Multiple APs recorded for hybrid electro-plasmonic stimulation. The reduction of current required to trigger APs with hybrid stimulation was up to 40% (Figure 5C), and cells stayed healthy longer after repeated exposure to hybrid stimulation compared to pure plasmonic stimulation. Insets of part (C) (i, ii, iii, and iv) show the separate traces of multiple APs individually for better visibility, as follows: (i) Prehybrid electrically evoked multiple APs (380 pA threshold); (ii) prehybrid electrically evoked shifts (200 pA); (iii) hybrid stimulation APs (250 pA, 35% below threshold); (iv) posthybrid electrically evoked APs.

stimulation was up to 40% lower, matching what was observed earlier with single AP recordings. This reinforces the previous findings above, supporting the effectiveness of the proposed platform for hybrid stimulation of neurons.

In this work, we have successfully demonstrated a safe and reproducible hybrid laser stimulation of primary trigeminal neurons using single and multiple pulses of visible light and electric currents. This was presented as an optimized technology platform for a hybrid electro-plasmonic modulation of neuron excitability using visible-light-sensitive gold nanotransducer particles. Gold nanoparticles were used to coat the plasmonic stimulation nanoelectrodes, since they are known to demonstrate the desired localized surface plasmon resonance effects and are biocompatible in multiple *in vivo* applications such as drug delivery, bioimaging, biosensors, *etc.*[25] LSPR fields are generated as a result of the strong surface interactions between the light and the conduction band electrons of the metal nanoparticles. A hybrid modulation neurodevice based on noncontact and nonmodification of neural interface approaches, using wireless SPR phenomena, is the ultimate solution for achieving enhanced spatial resolution and, thus, more clinically useful focal stimulation of neurons. It has the additional advantage of not generating excessive electrical artifacts that could interfere with concurrent neurophysiological recordings, currently used in electrical closed-loop neuroprosthetic systems for treating brain disease, hearing loss/deafness, and similar neurological disorders, as well as in experimental neuroscience.

The plasmonic oscillations in most metal nanoparticles occur mainly in the UV region. However, in the case of gold (Au), silver (Ag), and copper (Cu) nanoparticles, the plasmons shift nearer to the visible light domain, related to

https://dx.doi.org/10.1021/acsnano.0c00722
ACS Nano 2020, 14, 10917−10928

electrons in the s-atomic orbitals. Specifically, for gold nanoparticles, used in the present work, the SPR peak is around 520 nm, and it can be tuned with particle size and shape. The AuNPs are known to generate localized heating[26−28] due to SPR, called plasmonic heating. We used AuNPs of approximately 20 nm diameter and visible light at 532 nm, near the maximum position of the LSPR band in gold, to irradiate the AuNPs. It has been demonstrated that photosensitive AuNPs can be excited upon visible light irradiation and used to stimulate primary neurons and, more specifically, trigeminal neurons, without any genetic modifications or direct neural membrane surface contact. Compared to the currently predominant photothermal neuromodulation techniques using direct IR laser stimulation, which is susceptible to collateral heating, there is a fundamental difference in transduction. Au nanoparticles are the photoabsorbers, as opposed to water, nearby cells, or extracellular fluids, allowing heat distribution to be controlled and localized at submicron levels. With this approach, biomedical implants based on SPR phenomena have the potential to give better spatial resolution and thus more clinically useful focal stimulation. A hybrid modality is presented here, which adds small amounts of electric currents for cell stimulation, to overcome the issues with reproducibility, repeatability, and reliability as seen with pure optical stimulations. Hybrid stimulation significantly reduces the amount of current as compared to pure electrical stimulation (by ∼40%) as well as facilitates the firing of multiple APs. Further optimization experiments with different size/shape of gold nanoparticles and controlled deposition of layers on different types of nanoelectrodes could reduce current requirements further.

Electro-plasmonic prototypes based on the hybrid neuromodulation modes presented here have the potential to selectively inhibit or stimulate the electrical excitability of unmodified neurons depending on the specific needs. This can be achieved by varying the tunable electrical and optical stimulation input parameters of the individual inputs through fine-tuning and optimization of the hybrid stimulation (Figure 6). The fine-tuning of the electro-plasmonic stimulation sequence and variables (lead and lag time, intensity thresholds, duration) administered *via* short-duration (1−5 ms) repetitive pulsing of both electrical and optical stimuli, allowed for triggering repeatable multiple trains of action potential responses from the stimulated neurons, necessary for *in vivo* applications. It seems that short moderate power optical pulses in the milliseconds range are necessary for the successful activation of neurons. It is consistent with other studies using nanoparticles. Relatively high power light is employed by different laboratories in neuron activation studies (0.31 kW used by Carvalho-de-Souza *et al.*[4] or 1.5−5 kW used by Migliori *et al.*[29]), while relatively moderate power light is employed in inhibition studies (15 mW photothermal stimulation intensity used by Yoo *et al.*,[10] 57 mW used by Martino *et al.*,[30] or 120 mW used by Bazard *et al.*[22]). Also, a number of infrared neurostimulation (INS) studies[31] reported that short-wave IR pulses (few milliseconds) can stimulate neural fibers including retinal[32] and cortical neurons,[33,34] peripheral[19,35] and cranial nerves,[36−41] the central auditory system, and even cardiomyocytes[22] and neuroblastoma[22] cells. It has been reported that INS is mediated by rapid temperature transients induced by surroundings absorption[18,35,42] and that such transients can be induced with other types of photoabsorption as well, thus with visible light plasmonic stimulation as used in our study. It has been previously shown that the rapid temperature transients are directly accompanied by changes in cell membrane capacitance and mechanoelectric properties and resulting modulation of ionic membrane currents can lead to cell stimulation.[31] However, most previous optical/laser studies showed inhibition/modulation of spontaneous neural or cardiac activity, rather than excitation, whereas we show that exciting neurons is quite feasible with the hybrid stimulation approach. Furthermore, studies have been conducted using external photoresponsive materials such as gold nanoparticles, some needing genetic modification of the targeted cell, as mentioned above. Other approaches have been tried where plasma-membrane-targeted gold nanorods are prepared with a cationic protein/lipid complex to activate a thermosensitive cation channel, TRPV1, in intact neuronal cells.[20] The latter method provides an optogenetic platform without the need for prior genetic engineering of the target cells. In our study we use AuNPs coated on an external nanoelectrode, which does not need any bioconjugation or surface modification of the nanoneural interface to achieve the triggering of neural stimulation. Inhibition or activation is controlled by fine-tuning the hybrid input stimuli.

CONCLUSION

In this work, we demonstrated that a reduction of up to ∼40% of the input current threshold can be achieved for triggering APs, and cells stay healthy longer after repeated exposure to our hybrid stimulation platform. Survival rates greater than five times compared to pure plasmonic/optical stimulation is achieved. In addition, the cell's stimulation success rate was three times greater with the hybrid stimulation. We have shown that combining short-duration green visible light optical pulses with the complementary subthreshold level electric current pulses can reliably trigger a train of action potentials, possibly by activating ion channels in patterns like standard APs. Collectively, the combined hybrid stimulation input produced reliable APs related to more favorable membrane hyperpolarization. Nanomaterials, specifically gold, maximize the utility of thermal stimulation *via* surface plasmon resonance phenomena. The use of nanotechnology as a medium for photothermal stimulation has the potential to make way for noninvasive neural stimulators capable of cell-specific targeting, allowing for improved restoration of sensorimotor functions and removing side effects exhibited with current neuromodulation methods. Nanomaterials-enabled plasmonic stimulation, when paired with subthreshold electrical stimulation inputs in a tunable hybrid neuromodulation mode, could revolutionize the way neural or cardiac stimulation therapy is performed.

One good example is the cochlear implant technology and its applications, which after more than five decades still relies on electrical stimulation of the auditory nerves. Some of the latest advances in cochlear technology are based on bimodal solutions involving a cochlear implant and a hearing aid working together to give the patient a more natural hearing experience than just the traditional hearing aid or cochlear implant used alone.[43,44] However, this bimodal solution does not address the underlying cause for why cochlear implant users have difficulty hearing speech in background noise and suffer from poor music perception. Our hybrid neurostimulation findings, utilizing visible light for electro-plasmonic stimulation, provide opportunities to develop a next generation

https://dx.doi.org/10.1021/acsnano.0c00722
ACS Nano 2020, 14, 10917−10928

of high-acuity neural modulation prosthetic devices, tunable for the individual patient's needs.

MATERIALS AND METHODS

Gold Nanoelectrode Fabrication for Neuron Stimulation. Our first-generation AuNP-coated nanoelectrode system consisted of approximately 20 nm diameter colloidal AuNPs coated onto the surface of a glass micropipet, as reported in our previous work.[22] Briefly, colloidal AuNPs (spheres) were synthesized by a citrate method[22,45−48] that involves reduction of a gold salt solution (chloroauric acid, $HAuCl_4{\cdot}3H_2O$) by a sodium citrate ($Na_3C_6H_5O_7{\cdot}2H_2O$) aqueous solution. Spherical AuNPs with a 20 nm diameter were chosen because they are easily made with limited size dispersion into a colloidal solution and are generally considered to be biocompatible.[49] The method followed was the one described by Nath and Chilkoti,[50] who studied the interaction of a biomolecule with a monolayer of AuNPs-coated glass coverslips. The micropipet coating procedure involved three steps: (1) cleaning the glass surface, (2) functionalization of the glass surface with γ-(aminopropyl)-triethoxysilane, and (3) coating of the functionalized glass surface with colloidal AuNPs. We used this method in a similar manner for the current study to coat the synthesized AuNPs onto the borosilicate glass nanoelectrodes, with prior silanization of the glass pipet surface using a 10% volume solution of γ-(aminopropyl)triethoxysilane in ethanol. The silanized glass electrodes were dipped overnight at room temperature in the synthesized colloidal AuNP suspension, resulting in a self-arranged chemical deposition of AuNP coating onto the tip surface of the nanoelectrodes, which possess plasmonic properties.

Primary Neuron Cell Culture. Trigeminal neurons were obtained from the brain of 5−7-week-old C57B1/6 mice. The trigeminal neurons were removed after decapitation and maintained in a cold (4−5 °C) Ca^{2+}- and Mg^{2+}-free Hanks' balanced salt solution (HBSS; Gibco BRL, Rockville, MD, USA). Trigeminal neurons were dissociated enzymatically with HBSS containing collagenase type IA (1 mg mL^{-1}, Sigma, St. Louis, MO, USA) and Dispase II (1 mg mL^{-1}, Boehringer Mannheim, Mannheim, Germany). Enzymes, collagenase type 1 and Dispase II (2 mg/mL), were dissolved in HBSS and sterile filtered using a white PVDF syringe filter before use. The required solutions were prepared, 40 mL of HBSS, 21 mL of L15 + 10% FBS, and 11 mL of L15 + FBS. The tubes of L15 were placed in the incubator at 37 °C, 5% CO_2 to warm up. Meanwhile, a 20−40 g mouse was euthanized using CO_2 overdose and decapitated, and the trigeminal nerves were dissected out. The trigeminal ganglia were minced into pieces and left to incubate at 37 °C in the collagenase/Dispase II solution for 50 min. During this incubation, coated coverslips were transferred to a six-well plate. Coverslips were cleaned in 100% ethanol and then coated with a 5 μg/mL laminin mixed in poly D-lysine (PDL) coating solution. Coverslips were left at room temperature for at least 30 min. Then, the coating solution was aspirated with a pipet, and the coverslips were washed with 200 μL of sterile deionized (DI) water and allowed to dry before use. The Bunsen burner was set and three glass pipets were fire polished for trituration: large, medium (10−15 s to take up solution), and small (45−60 s to take up solution) size bores. After 30 min of incubation, the neurons are triturated with the wide-bore pipet and then put back into the 37 °C water bath for another 20 min. Finally, they were dissociated with the medium followed by the small-bore pipet. The cell suspension was then centrifuged at 2200 rpm for 2 min. A 55 μL amount of pen/strep solution (1:200) was added to the 11 mL of L15+FBS previously left in a 37 °C incubator. Next, the HBSS was aspirated and the pellet was resuspended in 10 mL of L-15 medium containing 10% FBS and centrifuged again (2200 rpm, 2 min). Medium was aspirated again, and cells were resuspended in 10 mL of L-15 medium containing 10% FBS and pen/strep and then centrifuged again (2200 rpm, 2 min). Finally, the medium was aspirated and cells were resuspended in 100 μL of L15+FBS+pen/strep (20 μL per coverslip). The suspension was pipetmixed 50 times with a p200 pipet and transferred in portions of 20 μL of suspension to coverslips coated with PDL and laminin. The six-well plate (culture dishes) was placed in an incubator for 1−2 h to incubate. Then, the wells were topped (flooded) with 2 mL of L15 containing 10% FBS and left to incubate at 37 °C. All cells were used within 36 h.

Plasmonic and Hybrid Optical Stimulation Method. For plasmonic and hybrid stimulations, the Au nanoparticle-coated nanoelectrode was placed adjacent (2 μm) to the cell, while the cell is patched in whole-cell current-clamp configuration using a micropipet equipped to measure the plasmonic responses. The 532 nm green laser (OBIS 532 nm laser, Coherent, Santa Clara, CA, USA) pulses were focused on the tip of the AuNPs-coated nanoelectrode through an optical fiber with a 50 μm inside diameter (custom fiber-optic cannula from ThorLabs). Electrical evoked action potentials were measured before and after optical stimulation. For hybrid stimulation, subthreshold electrical stimulus was added in addition to the optical stimulus. Cellular response was recorded using the patch-clamp system in whole-cell current-clamp configuration mode.

Whole-Cell Patch-Clamp Technique. The whole-cell patch-clamp technique was used in conjunction with a Multiclamp 700B amplifier and Digidata 1440 data acquisition interface system (Molecular Devices, Sunnyvale, CA, USA) and pCLAMP-9 software (Axon Instruments, Union City, CA, USA). The patch-clamp borosilicate glass pipet, having a resistance of 4−7 MΩ, was filled with an intracellular solution, using a microsyringe. The micropipets used for the patch-clamp recordings were pulled using a glass micropipet puller (P-97, from Sutter Instruments, Novato, CA, USA) by adjusting the pulling parameters to obtain 4−7 MΩ pipet resistance.[51] The pipet tip is placed in the bath filled with extracellular solution, and the tip focused under 20× magnification. To form a gigaseal, a small voltage pulse is applied (10 mV, 50 ms), and current responses recorded. The pipet is slowly lowered down. When very near to the cell, the movement is stopped, the pipet potential is zeroed, and a little suction is applied as needed to patch the cell and form a gigaseal (resistance >1 G-ohm). A membrane break-through was attempted by applying pressure to achieve the whole-cell configuration.

Extracellular Solution. Extracellular solution, used to flood the cells in the dish, was prepared with the following composition (mM): 154 NaCl; 4.7 KCl; 1.2 $MgCl_2$; 2.5 $CaCl_2$; 10 *N*-[2-hydroxyethyl]-piperazine-*N*′-[2-ethanesulfonic acid] (HEPES); the pH was adjusted between 7.3 and 7.5 with NaOH.

Intracellular Solution. Patch pipets (4−7 MΩ) were filled with an intracellular solution (mM): 140 KCl, 1 $CaCl_2$, 2 $MgCl_2$, 10 HEPES, 10 (D(+)-glucose, reagent ACS, anhydrous), 11 ethylene glycol-bis(β-aminoethyl ether)-*N*,*N*,*N*′,*N*′-tetraacetic acid; pH 7.3 adjusted with KOH. In current-clamp mode, holding membrane potential was maintained at −60 to −70 mV. Threshold (the most hyperpolarized potential at which the cell was able to fire an AP) was determined by injecting increments of depolarizing current (Δ of 50−100 pA) for 5 ms pulse width, until the cell started to elicit AP.

All the animal protocols and procedures were approved by the University of South Florida Institutional Animal Care and Use Committee (IACUC) and are consistent with U.S. Federal and NIH guidelines, with the necessary training provided.

AUTHOR INFORMATION

Corresponding Authors

Robert D. Frisina − *Department of Medical Engineering, Department of Communication Sciences and Disorders, College of Behavioral & Community Sciences, and Global Center of Hearing and Speech Research, University of South Florida, Tampa, Florida 33612, United States*; Email: rfrisina@usf.edu

Venkat R. Bhethanabotla − *Department of Medical Engineering, Department of Chemical & Biomedical Engineering, and Global Center of Hearing and Speech Research, University of South Florida, Tampa, Florida 33612, United States*; orcid.org/0000-0002-8279-0100; Email: bhethana@usf.edu

https://dx.doi.org/10.1021/acsnano.0c00722
ACS Nano 2020, 14, 10917−10928

Authors

Ratka Damnjanovic − *Department of Medical Engineering and Global Center of Hearing and Speech Research, University of South Florida, Tampa, Florida 33612, United States*

Parveen Bazard − *Department of Medical Engineering and Global Center of Hearing and Speech Research, University of South Florida, Tampa, Florida 33612, United States*

Complete contact information is available at: https://pubs.acs.org/10.1021/acsnano.0c00722

Author Contributions

R.D., P.B., R.D.F., and V.R.B. conceptualized and designed the research methodology and data interpretation. R.D.F. oversaw the neuron culture preparations. V.R.B. oversaw the physiology experiments. P.B. demonstrated and oversaw the nanoelectrode fabrication, patch-clamping technique and initial data recording. R.D. procured an additional manipulator and retrofitted the *in vitro* patch-clamp system accordingly. R.D. prepared the cell cultures, performed the experiments, and summarized the data. R.D. wrote and revised the manuscript with editorial contributions from P.B., R.D.F., and V.R.B.

Notes

The authors declare the following competing financial interest(s): A patent has been filed by University of South Florida.

ACKNOWLEDGMENTS

This work was partially supported by National Institutes of Health Grant P01 AG009524. Special thanks to Dr. P. K. Bahia from Prof. T. Taylor-Clark's Lab, College of Medicine Molecular Pharmacology & Physiology, University of South Florida in Tampa, USA, for their help in providing mouse tissue for trigeminal cell culture and for demonstrating the culturing technique.

REFERENCES

(1) Wang, Y.; Guo, L. Nanomaterial-Enabled Neural Stimulation. *Front. Neurosci.* **2016**, *10*, 69.

(2) Deisseroth, K. Optogenetics: 10 Years of Microbial Opsins in Neuroscience. *Nat. Neurosci.* **2015**, *18*, 1213−1225.

(3) Colombo, E.; Feyen, P.; Antognazza, M. R.; Lanzani, G.; Benfenati, F. Nanoparticles: A Challenging Vehicle for Neural Stimulation. *Front. Neurosci.* **2016**, *10*, 105.

(4) Carvalho-de-Souza, J. L.; Treger, J. S.; Dang, B.; Kent, S. B.; Pepperberg, D. R.; Bezanilla, F. Photosensitivity of Neurons Enabled by Cell-Targeted Gold Nanoparticles. *Neuron* **2015**, *86*, 207−217.

(5) Marino, A.; Arai, S.; Hou, Y.; Sinibaldi, E.; Pellegrino, M.; Chang, Y. T.; Mazzolai, B.; Mattoli, V.; Suzuki, M.; Ciofani, G. Piezoelectric Nanoparticle-Assisted Wireless Neuronal Stimulation. *ACS Nano* **2015**, *9*, 7678−7689.

(6) Chen, R.; Romero, G.; Christiansen, M. G.; Mohr, A.; Anikeeva, P. Wireless Magnetothermal Deep Brain Stimulation. *Science* **2015**, *347*, 1477−1480.

(7) Eom, K.; Kim, J.; Choi, J. M.; Kang, T.; Chang, J. W.; Byun, K. M.; Jun, S. B.; Kim, S. J. Enhanced Infrared Neural Stimulation Using Localized Surface Plasmon Resonance of Gold Nanorods. *Small* **2014**, *10*, 3853−3857.

(8) Yong, J.; Needham, K.; Brown, W. G.; Nayagam, B. A.; McArthur, S. L.; Yu, A.; Stoddart, P. R. Gold-Nanorod-Assisted Near-Infrared Stimulation of Primary Auditory Neurons. *Adv. Healthcare Mater.* **2014**, *3*, 1862−1868.

(9) Chen, S.; Weitemier, A. Z.; Zeng, X.; He, L.; Wang, X.; Tao, Y.; Huang, A. J. Y.; Hashimotodani, Y.; Kano, M.; Iwasaki, H.; Parajuli, L. K.; Okabe, S.; Teh, D. B. L.; All, A. H.; Tsutsui-Kimura, I.; Tanaka, K. F.; Liu, X.; McHugh, T. J. Near-Infrared Deep Brain Stimulation *via* Upconversion Nanoparticle-Mediated Optogenetics. *Science* **2018**, *359*, 679−684.

(10) Yoo, S.; Hong, S.; Choi, Y.; Park, J. H.; Nam, Y. Photothermal Inhibition of Neural Activity with Near-Infrared-Sensitive Nanotransducers. *ACS Nano* **2014**, *8*, 8040−8049.

(11) Li, W.; Luo, R.; Lin, X.; Jadhav, A. D.; Zhang, Z.; Yan, L.; Chan, C. Y.; Chen, X.; He, J.; Chen, C. H.; Shi, P. Remote Modulation of Neural Activities *via* Near-Infrared Triggered Release of Biomolecules. *Biomaterials* **2015**, *65*, 76−85.

(12) Pappas, T. C.; Wickramanyake, W. M.; Jan, E.; Motamedi, M.; Brodwick, M.; Kotov, N. A. Nanoscale Engineering of a Cellular Interface with Semiconductor Nanoparticle Films for Photoelectric Stimulation of Neurons. *Nano Lett.* **2007**, *7*, 513−519.

(13) Duke, A. R.; Cayce, J. M.; Malphrus, J. D.; Konrad, P.; Mahadevan-Jansen, A.; Jansen, E. D. Combined Optical and Electrical Stimulation of Neural Tissue *In Vivo*. *J. Biomed. Opt.* **2009**, *14*, 060501.

(14) Zhao, Y.; Larimer, P.; Pressler, R. T.; Strowbridge, B. W.; Burda, C. Wireless Activation of Neurons in Brain Slices Using Nanostructured Semiconductor Photoelectrodes. *Angew. Chem., Int. Ed.* **2009**, *48*, 2407−2410.

(15) Parameswaran, R.; Carvalho-de-Souza, J. L.; Jiang, Y.; Burke, M. J.; Zimmerman, J. F.; Koehler, K.; Phillips, A. W.; Yi, J.; Adams, E. J.; Bezanilla, F. Photoelectrochemical Modulation of Neuronal Activity with Free-standing Coaxial Silicon Nanowires. *Nat. Nanotechnol.* **2018**, *13*, 260.

(16) Rettenmaier, A.; Lenarz, T.; Reuter, G. Nanosecond Laser Pulse Stimulation of Spiral Ganglion Neurons and Model Cells. *Biomed. Opt. Express* **2014**, *5*, 1014−1025.

(17) Zhang, J.; Atay, T.; Nurmikko, A. V. Optical Detection of Brain Cell Activity Using Plasmonic Gold Nanoparticles. *Nano Lett.* **2009**, *9*, 519−524.

(18) Shapiro, M. G.; Homma, K.; Villarreal, S.; Richter, C.-P.; Bezanilla, F. Infrared Light Excites Cells by Changing Their Electrical Capacitance. *Nat. Commun.* **2012**, *3*, 736.

(19) Wells, J.; Kao, C.; Mariappan, K.; Albea, J.; Jansen, E. D.; Konrad, P.; Mahadevan-Jansen, A. Optical Stimulation of Neural Tissue *In Vivo*. *Opt. Lett.* **2005**, *30*, 504−506.

(20) Nakatsuji, H.; Numata, T.; Morone, N.; Kaneko, S.; Mori, Y.; Imahori, H.; Murakami, T. Thermosensitive Ion Channel Activation in Single Neuronal Cells by Using Surface-Engineered Plasmonic Nanoparticles. *Angew. Chem., Int. Ed.* **2015**, *54*, 11725−11729.

(21) Eom, K.; Byun, K. M.; Jun, S. B.; Kim, S. J.; Lee, J. Theoretical Study on Gold-Nanorod-Enhanced Near-Infrared Neural Stimulation. *Biophys. J.* **2018**, *115*, 1481−1497.

(22) Bazard, P.; Frisina, R. D.; Walton, J. P.; Bhethanabotla, V. R. Nanoparticle-Based Plasmonic Transduction for Modulation of Electrically Excitable Cells. *Sci. Rep.* **2017**, *7*, 7803.

(23) Rea, P. *Essential Clinical Anatomy of the Nervous System. Ch1: Introduction to the Nervous System*; Elsevier/AP: Amsterdam; Boston, 2015; pp 25−27.

(24) Waldman, S. D. *Pain Management E-Book*, 2nd ed.; Elsevier Health Sciences: Philadelphia, PA, 2011; pp 1145−1151.

(25) Lewinski, N.; Colvin, V.; Drezek, R. Cytotoxicity of Nanoparticles. *Small* **2008**, *4*, 26−49.

(26) Coronado, E. A.; Encina, E. R.; Stefani, F. D. Optical Properties of Metallic Nanoparticles: Manipulating Light, Heat and Forces at the Nanoscale. *Nanoscale* **2011**, *3*, 4042−4059.

(27) Huang, X.; El-Sayed, M. A. Gold Nanoparticles: Optical Properties and Implementations in Cancer Diagnosis and Photothermal Therapy. *J. Adv. Res.* **2010**, *1*, 13−28.

(28) Horikoshi, S., Serpone, N. Microwaves in Nanoparticle Synthesis: Fundamentals and Applications. In *Microwaves in Nanoparticle Synthesis: Fundamentals and Applications*; Horikoshi, S., Serpone, N., Eds.; John Wiley & Sons, Wiley-VCH Verlag GmbH & Co. KGaA: Weinheim, Germany, 2013; pp 1−24.

(29) Migliori, B.; Di Ventra, M.; Kristan, W., Jr Photoactivation of Neurons by Laser-Generated Local Heating. *AIP Adv.* **2012**, *2*, 032154.

(30) Martino, N.; Feyen, P.; Porro, M.; Bossio, C.; Zucchetti, E.; Ghezzi, D.; Benfenati, F.; Lanzani, G.; Antognazza, M. R. Photothermal Cellular Stimulation in Functional Bio-Polymer Interfaces. *Sci. Rep.* **2015**, *5*, 8911.
(31) Plaksin, M.; Shapira, E.; Kimmel, E.; Shoham, S. Thermal Transients Excite Neurons through Universal Intramembrane Mechanoelectrical Effects. *Phys. Rev. X* **2018**, *8*, 011043.
(32) Bec, J. M.; Albert, E. S.; Marc, I.; Desmadryl, G.; Travo, C.; Muller, A.; Chabbert, C.; Bardin, F.; Dumas, M. Characteristics of Laser Stimulation by Near-Infrared Pulses of Retinal and Vestibular Primary Neurons. *Lasers Surg. Med.* **2012**, *44*, 736−745.
(33) Cayce, J. M.; Friedman, R. M.; Chen, G.; Jansen, E. D.; Mahadevan-Jansen, A.; Roe, A. W. Infrared Neural Stimulation of Primary Visual Cortex in Non-Human Primates. *NeuroImage* **2014**, *84*, 181−190.
(34) Cayce, J. M.; Friedman, R. M.; Jansen, E. D.; Mahavaden-Jansen, A.; Roe, A. W. Pulsed Infrared Light Alters Neural Activity in Rat Somatosensory Cortex *In Vivo*. *NeuroImage* **2011**, *57*, 155−166.
(35) Wells, J.; Kao, C.; Konrad, P.; Milner, T.; Kim, J.; Mahadevan-Jansen, A.; Jansen, E. D. Biophysical Mechanisms of Transient Optical Stimulation of Peripheral Nerve. *Biophys. J.* **2007**, *93*, 2567−2580.
(36) Izzo, A. D.; Richter, C. P.; Jansen, E. D.; Walsh, J. T., Jr Laser Stimulation of the Auditory Nerve. *Lasers Surg. Med.* **2006**, *38*, 745−753.
(37) Littlefield, P. D.; Vujanovic, I.; Mundi, J.; Matic, A. I.; Richter, C. P. Laser Stimulation of Single Auditory Nerve Fibers. *Laryngoscope* **2010**, *120*, 2071−2082.
(38) Teudt, I. U.; Nevel, A. E.; Izzo, A. D.; Walsh, J. T., Jr; Richter, C. P. Optical Stimulation of the Facial Nerve: A New Monitoring Technique? *Laryngoscope* **2007**, *117*, 1641−1647.
(39) Izzo, A. D.; Walsh, J. T., Jr; Ralph, H.; Webb, J.; Bendett, M.; Wells, J.; Richter, C.-P. Laser Stimulation of Auditory Neurons: Effect of Shorter Pulse Duration and Penetration Depth. *Biophys. J.* **2008**, *94*, 3159−3166.
(40) Richter, C.-P.; Rajguru, S. M.; Matic, A. I.; Moreno, E. L.; Fishman, A. J.; Robinson, A. M.; Suh, E.; Walsh, J. T., Jr Spread of Cochlear Excitation During Stimulation with Pulsed Infrared Radiation: Inferior Colliculus Measurements. *J. Neural Eng.* **2011**, *8*, 056006.
(41) Rajguru, S. M.; Richter, C. P.; Matic, A. I.; Holstein, G. R.; Highstein, S. M.; Dittami, G. M.; Rabbitt, R. D. Infrared Photostimulation of the Crista Ampullaris. *J. Physiol.* **2011**, *589*, 1283−1294.
(42) Farah, N.; Brosh, I.; Butson, C. R.; Shoham, S. *Photo-Thermal Neural Excitation by Extrinsic and Intrinsic Absorbers: A Temperature-Rate Model*. 2012, arXiv:1201.4617v1. Neurons and Cognition. https://arxiv.org/abs/1201.4617 (accessed January 15, 2020).
(43) Dorman, M. F.; Gifford, R. H.; Spahr, A. J.; McKarns, S. A. The Benefits of Combining Acoustic and Electric Stimulation for the Recognition of Speech, Voice and Melodies. *Audiol. Neuro-Otol.* **2008**, *13*, 105−112.
(44) Wolfe, J.; Morais, M.; Schafer, E. Speech Recognition of Bimodal Cochlear Implant Recipients Using a Wireless Audio Streaming Accessory for the Telephone. *Otol. Neurotol.* **2016**, *37*, e20−e25.
(45) Alshammari, A.; Köckritz, A.; Kalevaru, V. N.; Bagabas, A.; Martin, A. Influence of Single Use and Combination of Reductants on the Size, Morphology and Growth Steps of Gold Nanoparticles in Colloidal Mixture. *Open J. Phys. Chem.* **2012**, *2*, 252−261.
(46) Tyagi, H.; Kushwaha, A.; Kumar, A.; Aslam, M. A Facile pH Controlled Citrate-Based Reduction Method for Gold Nanoparticle Synthesis at Room Temperature. *Nanoscale Res. Lett.* **2016**, *11*, 362.
(47) Kimling, J.; Maier, M.; Okenve, B.; Kotaidis, V.; Ballot, H.; Plech, A. Turkevich Method for Gold Nanoparticle Synthesis Revisited. *J. Phys. Chem. B* **2006**, *110*, 15700−15707.
(48) Turkevich, J.; Stevenson, P. C.; Hillier, J. A Study of the Nucleation and Growth Processes in the Synthesis of Colloidal Gold. *Discuss. Faraday Soc.* **1951**, *11*, 55−75.
(49) Shukla, R.; Bansal, V.; Chaudhary, M.; Basu, A.; Bhonde, R. R.; Sastry, M. Biocompatibility of Gold Nanoparticles and Their Endocytotic Fate Inside the Cellular Compartment: A Microscopic Overview. *Langmuir* **2005**, *21*, 10644−10654.
(50) Nath, N.; Chilkoti, A. A Colorimetric Gold Nanoparticle Sensor to Interrogate Biomolecular Interactions in Real Time on a Surface. *Anal. Chem.* **2002**, *74*, 504−509.
(51) Oesterle, A. Pipette Cookbook 2018: P-97 & P-1000 Micropipette Pullers. In *Sutter Instrument Company* [Online]; Oesterle, A., Ed.; Novato, CA, 2015; pp 5−33; https://www.sutter.com/PDFs/pipette_cookbook.pdf (accessed January 15, 2020).

https://dx.doi.org/10.1021/acsnano.0c00722
ACS Nano 2020, 14, 10917−10928